INTERNATIONAL ATOMIC ENERGY AGENCY
UNITED NATIONS EDUCATIONAL, SCIENTIFIC AND CULTURAL ORGANIZATION

INTERNATIONAL CENTRE FOR THEORETICAL PHYSICS
34100 TRIESTE (ITALY) - P.O.B. 586 - MIRAMARE - STRADA COSTIERA 11 - TELEPHONE: 2240-1
CABLE: CENTRATOM - TELEX 460392 - I

H4.SMR/303-11

WORKSHOP
GLOBAL GEOPHYSICAL INFORMATICS WITH APPLICATIONS TO RESEARCH IN EARTHQUAKE PREDICTIONS AND REDUCTION OF SEISMIC RISK

(15 November - 16 December 1988)

ANALYSIS OF SEISMIC INSTABILITY OF THE VANCOUVER ISLAND LITHOPROBE TRANSECT

E. NYLAND & QING LI

University of Alberta
Dept. of Physics
Edmonton T6G 2J1
Canada

Analysis of seismic instability of the Vancouver Island lithoprobe transect

E. NYLAND AND QING LI
Department of Physics, University of Alberta, Edmonton, Alta., Canada T6G 2J1

Received January 28, 1986
Revision accepted May 16, 1986

Seismic refraction and reflection surveys and gravity measurements over Vancouver Island, British Columbia, Canada, can constrain a finite-element model of the geodynamics of the subduction zone. Stress estimates obtained from this model have been combined with rock failure criteria to yield a probability measure of seismic risk that assumes seismic events start from a dilute distribution of Griffith cracks. The results are in agreement with the observed seismicity and lead to the suggestion that the dominant mechanism of this oceanic plate subduction zone is gravitational ridge push and mantle convection.

Des levés de sismique réfraction et réflexion et des mesures de gravimétrie au-dessus de l'île Vancouver, Colombie-Britannique, Canada, permettent d'élaborer un modèle par éléments finis de la géodynamique d'une zone de subduction. Les contraintes estimées à l'aide de ce modèle ont été combinées avec les critères de fissuration de la roche dans la but d'obtenir une mesure de probabilité de risque sismique, en supposant que les événements sismiques soient amorcés par une distribution élargie des fissures de Griffith. Les résultats sont en accord avec la sismicité observée et suggèrent que le mécanisme dominant dans cette zone de subduction de la plaque océanique est la poussée gravitationnelle d'une crête et la convection dans le manteau.

[Traduit par la revue]

Can. J. Earth Sci. 23, 2057 – 2067 (1986)

Introduction

Seismic experiments and gravity data on Vancouver Island strongly support geological contentions that the British Columbia margin is a subduction zone (Riddihough 1977; Keen and Hyndman 1979; R. A. Stacey 1973). The tectonic regime of the continental margin of western Canada (Fig. 1) is dominated by three lithospheric plates: the Pacific plate, the America plate, and the Juan de Fuca plate. The small northern part of the Juan de Fuca plate moves independently and has been named the Explorer plate. The boundary between the Pacific and the America plates is the Queen Charlotte transform fault, which lies along the edge of the continental shelf from the southern edge of the Queen Charlotte Islands to southern Alaska. The motion on this fault is right lateral, at about 5.5 cm/year. The Explorer – Pacific and Juan de Fuca – Pacific boundaries are defined by numerous en échelon spreading axes, offset by short transform segments. The present rate of motion across these boundaries ranges from about 4 to 6 cm/year (full spreading rate). The boundary between the Juan de Fuca and the Explorer plates is the Nootka fracture zone, a strike-slip fault with left lateral motion of about 2 cm/year.

The boundary between the America plate and the Juan de Fuca and Explorer plates is a zone of convergence or subduction, with underthrusting probably starting near the base of the continental slope at rates from 2 to 4.5 cm/year (Riddihough 1984; Keen and Hyndman 1979). That subduction has

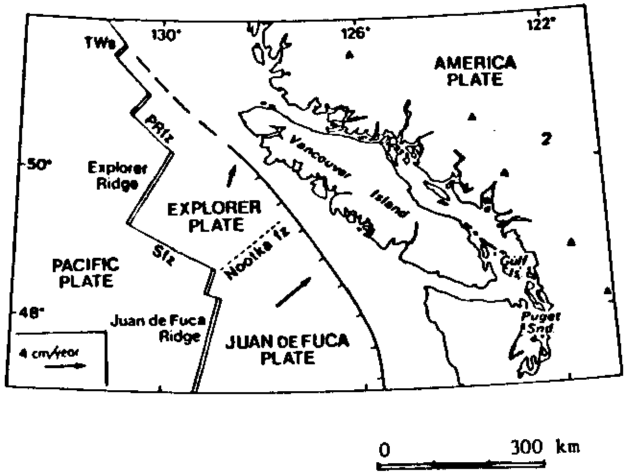

FIG. 1. Tectonic map of western Canada showing the main lithosphere plate boundaries and relative plate motion.

Printed in Canada / Imprimé au Canada

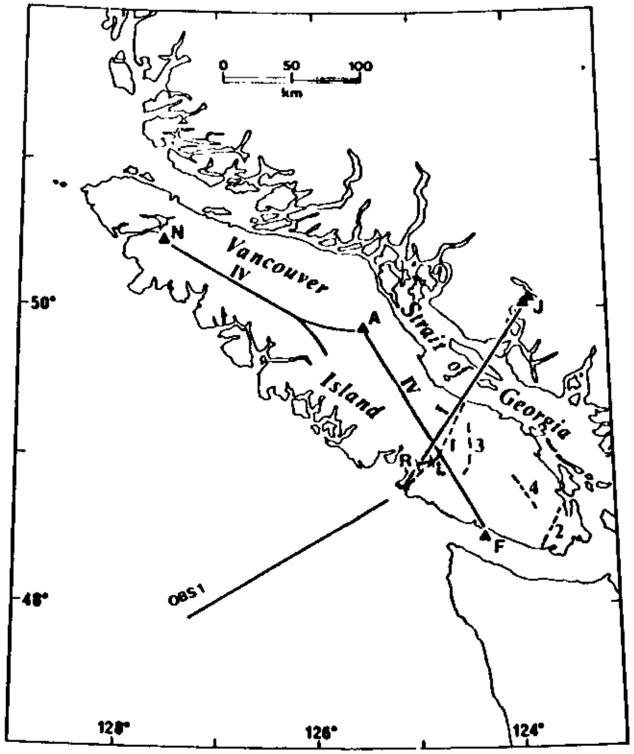

FIG. 2. Locations of seismic lines in VISP1980 denoted by solid rule; lithoprobe seismic profiles are denoted by broken rule.

occurred on the boundaries between the Juan de Fuca and Explorer plates and the America plate during the past few million years is well established. Doubts as to whether it is continuing at present arise primarily from the lack of a deep margin trench, from the lack of deep earthquakes, and from the lack of observed thrust mechanisms beneath the continental slope and shelf.

The updated results of the spreading rate and direction of movement of the plates in this area from Riddihough (1984) showed that the Juan de Fuca plate has moved in a direction about N40°E relative to the America plate for the last 65 Ma. The direction of movement of the Explorer plate relative to the America plate has changed to about N10°E at present. The convergence rate of the subduction of the northern part of the Vancouver Island continental margin has changed from 6 cm/year, 6.5 Ma ago, to about 2.3 cm/year at present. In the northern part, it has changed from 6.5 cm/year to about 4.4 cm/year.

Seismic data (Fig. 2) can constrain structures in this area. McMechan and Spence (1983) combined the results of seismic line IV with gravity results and presented three laterally homogeneous models of the crust and upper mantle (Fig. 3). The upper 20 km of their structure is well constrained by the two reversed profiles NA and AF. The structure of the lower crust and upper mantle is only weakly constrained; each of the three models fits certain travel-time and (or) amplitude observations better than others. However, model 2, which contains a low velocity zone and a low upper mantle velocity of 7.5 km/s at 37 km, is their preferred interpretation. The actual structure may vary laterally, being nearer model 1 beneath the north half of Vancouver Island and nearer model 2 beneath the south.

On line I (Fig. 2), a two-dimensional model (Fig. 4) results from a trial and error application of a ray-tracing technique (Ellis *et al.* 1983). The two-dimensional ray-trace model is constrained by the model of McMechan and Spence (1983) at the intersection with line IV (Fig. 2). The Moho west of the central portion of Vancouver Island appears to dip near 6° toward the continent, whereas that in the east is essentially flat lying. The gravity models (Riddihough 1979; J. F. Sweeney, personal communication, 1985) are generally consistent west of the central portion of Vancouver Island. The position at which the continental crust suddenly thickens beneath the central part of Vancouver Island corresponds fairly closely to the position in Riddihough's model where the subducting litho-

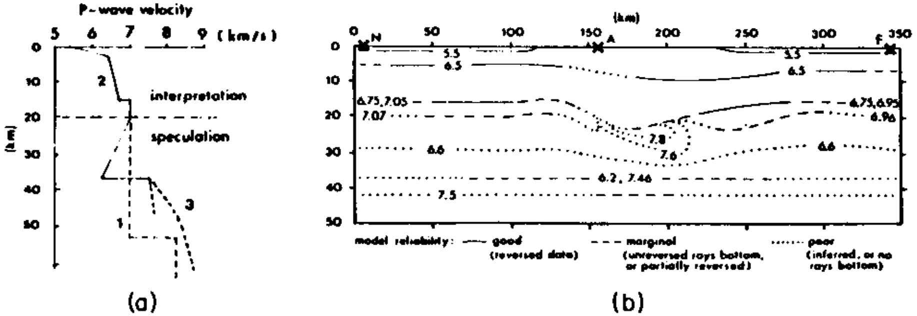

FIG. 3. (*a*) Three models corresponding to the left end of (*b*). (*b*) Two-dimensional velocity distribution along profile shown in Fig. 2. Modified from McMechan and Spence (1983).

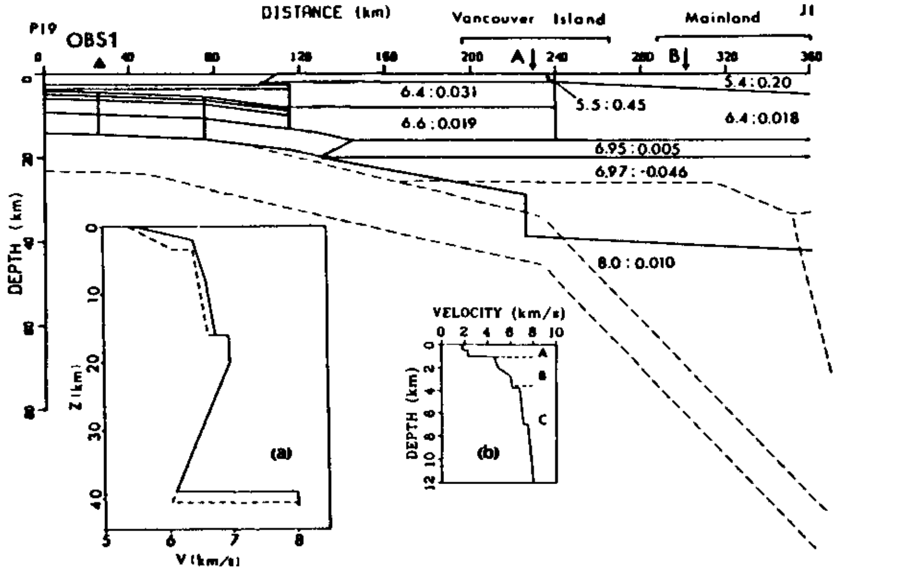

FIG. 4. Two-dimensional structure determined by ray tracing. Insert (*a*) shows velocity–depth models at locations A (solid line) and B (dashed line); insert (*b*), at location OBS1. Modified from Ellis *et al.* (1983).

sphere dramatically increases its dip. The presence of the Moho in the ray-trace model at about 40 km depth emphasizes the existence of a seismic discontinuity where no comparable density discontinuity is present in the gravity model.

The reflection lines also indicated the 15.5 km reflector of McMechan and Spence (1983). The reflector at 24 km depth, for which no corresponding boundary exists in the refraction models, indicates the upper boundary of subducting oceanic lithosphere at this depth. The possible reflector near 36 km corresponds reasonably well to the base of the subducting oceanic lithosphere. Furthermore, the dip of 5° corresponds closely to the dip of about 6° proposed by the Riddihough (1979) model and the refraction models.

Preliminary analysis of lithoprobe seismic profiles (Yorath *et al.* 1985; Green *et al.* 1986*a*, 1986*b*) shows a strong reflection, probably the top of the underthrusting oceanic crust (Fig. 5), about 20 km beneath the west coast of the island and 31 km beneath the east coast. Toward the northern end of VISP1, there is some evidence for an increase in dip of the reflector, beyond which continuity is lost. The apparent

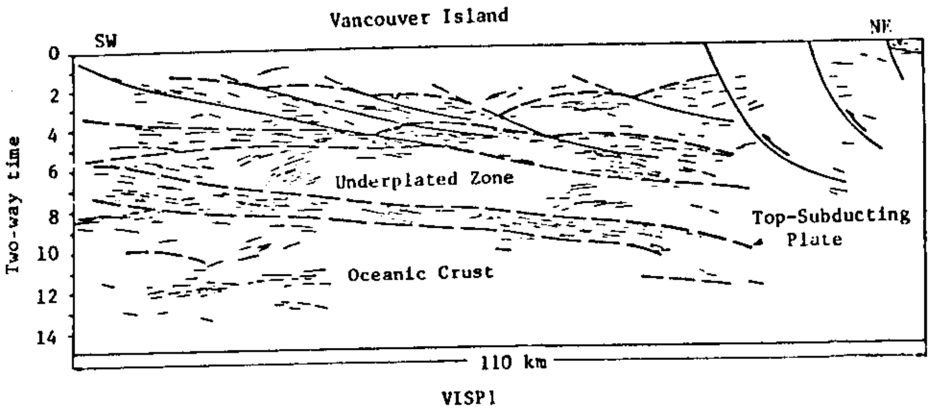

FIG. 5. Preliminary interpretation of lithoprobe VISP1. Modified from Yorath *et al.* (1985).

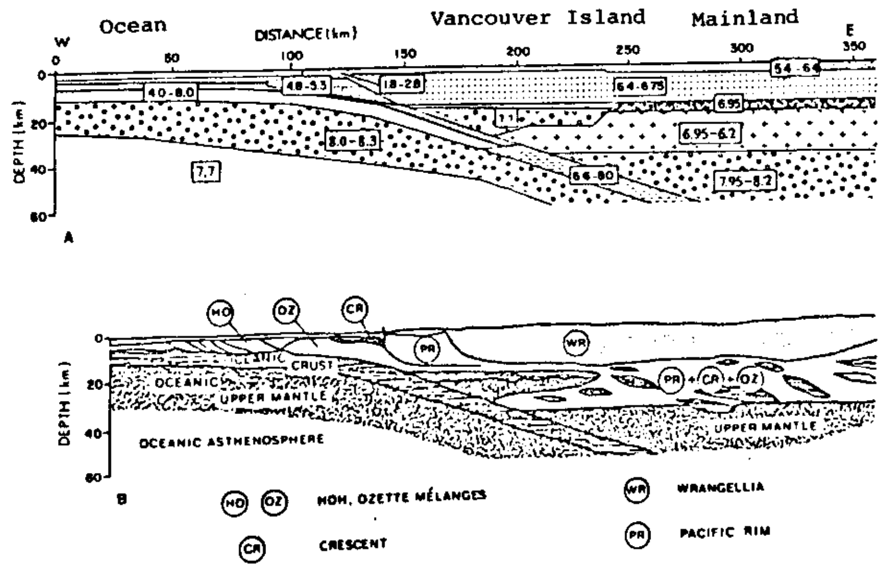

FIG. 6. Velocity model and tectonic cross section across the continental margin. Modified from Yorath *et al.* (1985).

absence of the deepest reflections beneath the northernmost region of VISP1 has two possible explanations. Perhaps it is related in some way to geological and topographical complexities, because the profile transverses the nose of a northwest–southeast-trending anticlinal ridge, but it may also be that the dip of the subducting plate increases suddenly to a value in excess of 45°. Relatively conventional data processing would have filtered out any reflections from such a zone. Above this reflector, a region with high density or high velocity or both has led to the suggestion that it represents an underplated slab of oceanic lithosphere, perhaps a remnant of an earlier phase of subduction. This underplated slab corresponds to the large block of anomalous material in the gravity model (Green *et al.* 1986*a*, 1986*b*) (Fig. 6).

Most of the seismicity (Fig. 7) on the western Canada margin has been concentrated along the three major plate boundaries: the Queen Charlotte – Fairweather fault system (Pacific–America plates), the offshore ridge – fracture zone

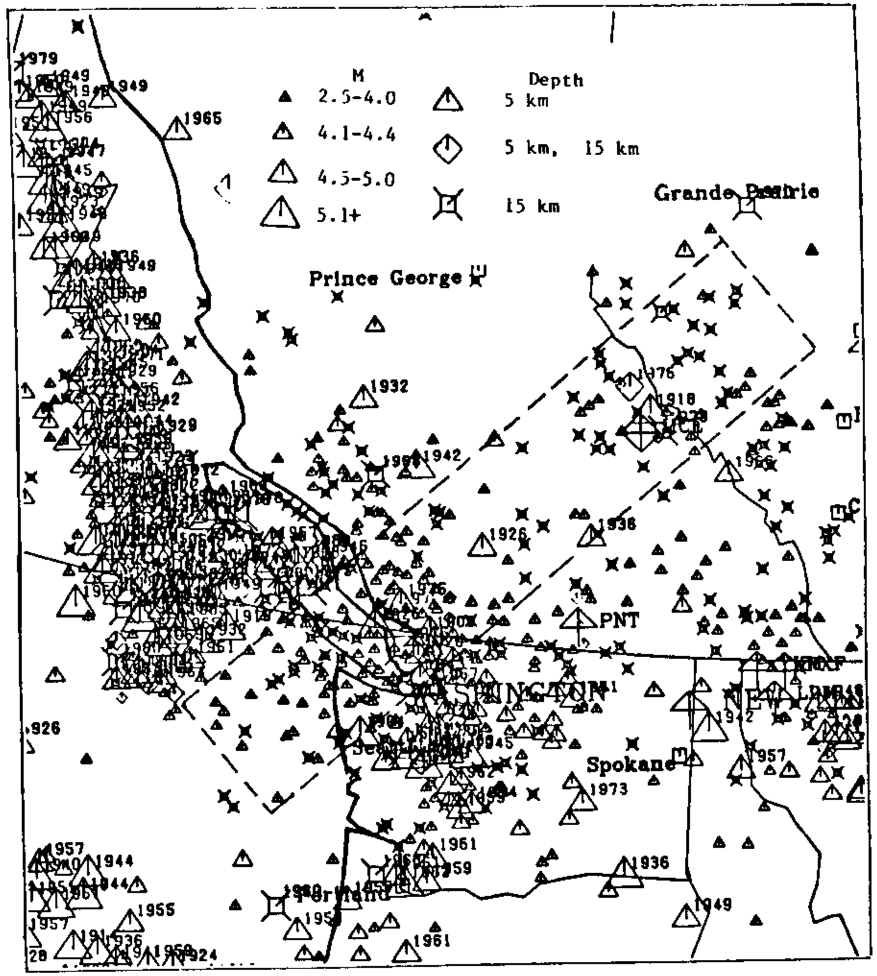

FIG. 7. Earthquake epicentres of the western Canadian margin. The area in the rectangle is studied in this paper.

system (Pacific – Juan de Fuca plates), and the Vancouver Island – Puget Sound region (Juan de Fuca – America plates) (Milne *et al.* 1978). Those earthquakes in the rectangle for which depths were available were projected onto a cross section (Fig. 8). Earthquakes associated with the Queen Charlotte fault, the ocean ridge system, and the Puget Sound region may be in different stress environments from those in Vancouver Island. Fault mechanism solutions (Rogers 1979) show predominantly strike-slip, either dextral slip to the northwest or sinistral slip to the northeast.

Model of the Vancouver Island subduction zone

In the top few kilometres, where the temperature does not exceed 300°C, the lithosphere can be thought of as an elastic layer over a high viscosity layer (T. Lewis, personal communication, 1985). Below this temperature, the thermal stress is small and the tectonics can be described by elastic stress (Turcotte 1974). Young's modulus E should become smaller as depth increases because the material is becoming more ductile as temperature increases. Kirby (1977) suggested an exponential decay of the Young's modulus E with temperature:

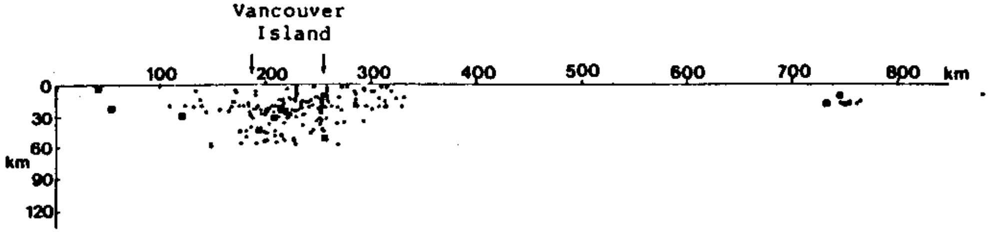

FIG. 8. Distribution of foci of earthquakes within rectangle in Fig. 7.

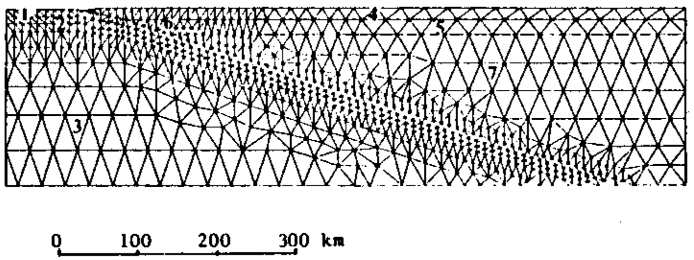

FIG. 9. Nodal distribution and structure of the finite-element model. Material index numbers are shown in Table 1.

$$E = E_{min} + E_0 e^{-x}$$

where $x = T^2/C$; T is temperature; $C = 600°C$; and E_0 and E_{min} are material constants.

Wiens (1983) showed that seismicity is limited to formations below 700–800°C. The limiting temperature for seismicity in shallow seismic slabs is about 600°C (Molnar *et al.* 1979).

The elastic lithosphere thickness is usually derived from the response of the lithosphere to long-term loads and agrees with the seismically active thickness of the lithosphere (Watts *et al.* 1980), whereas the seismic thickness (taken from its response to short-term loads) is about twice the elastic thickness (Leeds *et al.* 1974). Earthquakes occur primarily in areas of the lithosphere that can sustain long-term loads as identified by studies of flexure. Because estimates of elastic thickness computed by assuming a "seismic" Young's modulus E give the result that the elastic thickness is slightly less (about 10%) than the seismically active thickness (Watts *et al.* 1980; Wiens and Stein 1983), we suggest that the geodynamic Young's modulus should be 20% smaller than the "seismic" one.

The finite-element model we designed lies on a line crossing Vancouver Island and perpendicular to the coast of North America (Fig. 9). Because the Juan de Fuca plate has moved in a direction N35°E relative to the America plate for the last million years, we assumed the driving force on the Juan de Fuca plate would be in this direction. In the model, the subducting plate dips at 10° from the base of the continental slope, then the dip increases to 18° and continues at this angle down 200 km. The shallow dip part of the model is constrained by the seismic refraction profile (Ellis *et al.* 1983). Beneath Vancouver Island, the dip of the sinking slab can be constrained by

TABLE 1. Parameters of the model

Index of materials	Compressive velocity (km/s)	Young's modulus ($\times 10^{11}$ dyn/cm²)	Poisson ratio	Density (g/cm³)
1	7.0	0.954	0.25	2.92
2	8.2	1.335	0.3	3.34
3	7.7	1.039	0.3	2.295
4	6.75	0.887	0.25	2.92
5	6.4	0.711	0.3	2.92
6	7.7	1.163	0.3	3.30
7	8.0	1.249	0.3	3.285

the data from onshore and offshore seismic refraction and reflection surveys. The shallow part of the model is also consistent with the gravity data. The deep parts of the model are weakly constrained because of the absence of deep reflections.

The material parameters used (Table 1) include elastic moduli. For most crustal rocks, Poisson's ratio is around 0.25; it is a common assumption in geophysical modelling to use 0.25 and 0.3 for Poisson's ratio. In this model, therefore, 0.25 is used for surface rocks, and 0.3 is used for the rocks in the lower layer of the plate. The values for the density are inferred from the gravity model (J. F. Sweeney, personal communication, 1985). With Poisson's ratio and density determined as above, Young's modulus can be calculated from the compression wave velocity. This calculation gives the value for short-term load response. As discussed above, we subtract 20% from this E to get the static modulus we need.

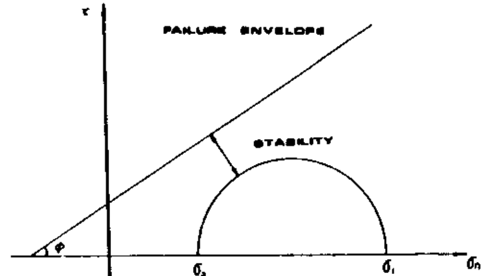

FIG. 10. General definition of instability: the minimum distance from the surface of the Mohr circle to the failure criterion.

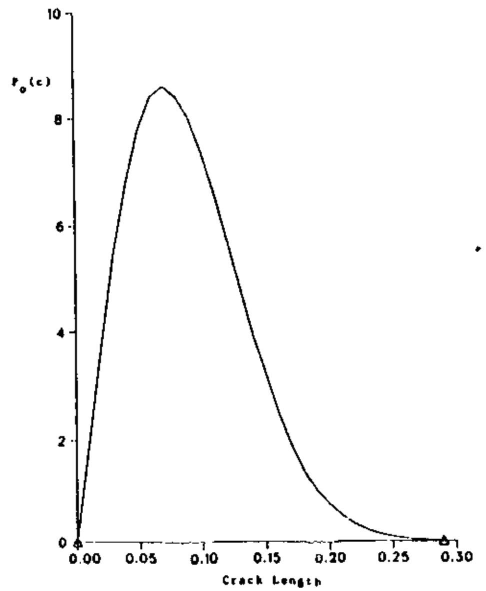

FIG. 11. Assumed distribution of cracks in a body. $P_0(c)$ is calculated for $\sigma = 0.1$; c is normalized with the choice of σ.

Gravitational pull of a dense subducted slab at an island arc, gravitational sliding or pushing from ocean ridges, viscous drag due to convection currents in the asthenosphere, frictional forces acting on the fault plane of thrust earthquakes at subduction zones and of strike-slip earthquakes along transform faults, and viscous resistance due to the asthenosphere are forces that affect plate motion (Kanamori 1980). The implicit assumption made here is that the lack of seismicity along the boundary implies strong continent–plate coupling. A thermal convection model suggests (F. D. Stacey 1977) the value of the

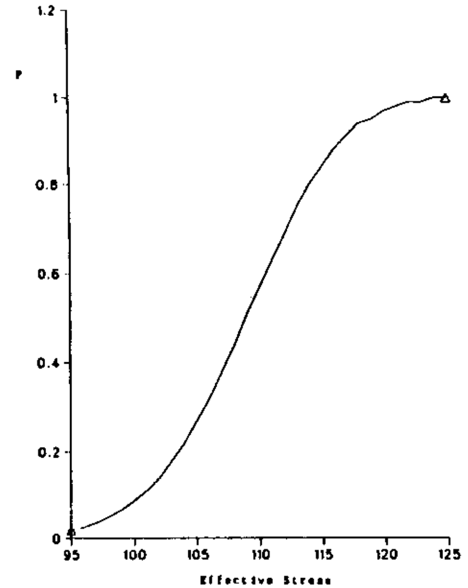

FIG. 12. Probability function of P, which is calculated for $\lambda^2/\sigma^2 = 7 \times 10^6$; $n = 100$.

viscous stress τ is about 15×10^5 Pa (15 bar). Ridge-push forces are about 200×10^5 Pa (200 bar) (McKenzie 1969), and because they are balanced by viscous drag, we introduce them as body forces rather than boundary tractions. This force will balance the viscous drag and the friction at plate boundaries and keep the plate moving steadily.

Stability calculation

A two-dimensional problem such as this is conveniently visualized with a Mohr circle representation. We assume brittle failure in which the critical shear stress that is required for failure is

$$\tau = S_0 + \sigma_n \tan \phi$$

where S_0 and ϕ are material constants; and σ_n is the pressure on the failure plane. S_0, the shear strength under zero normal pressure, varies from zero in fractured materials to about 50×10^5 Pa (50 bar) for sedimentary rocks and up to several hundred bars for igneous and intact materials. ϕ is the angle of shear resistance, which lies between 20 and 45°. Failure occurs when the Mohr circle for the stress touches the Mohr–Coulomb envelope.

The stability at some location in the model is the minimum distance between the failure envelope and the Mohr circle of the stress state at the position (Fig. 10) (Li 1986). The farther the Mohr circle is from the failure envelope, the more stable is the stress state. We use effective shear stress $(|\tau| - \sigma_n \tan \phi)$ and the concept of a Griffith crack to develop a measure of risk of seismic failure.

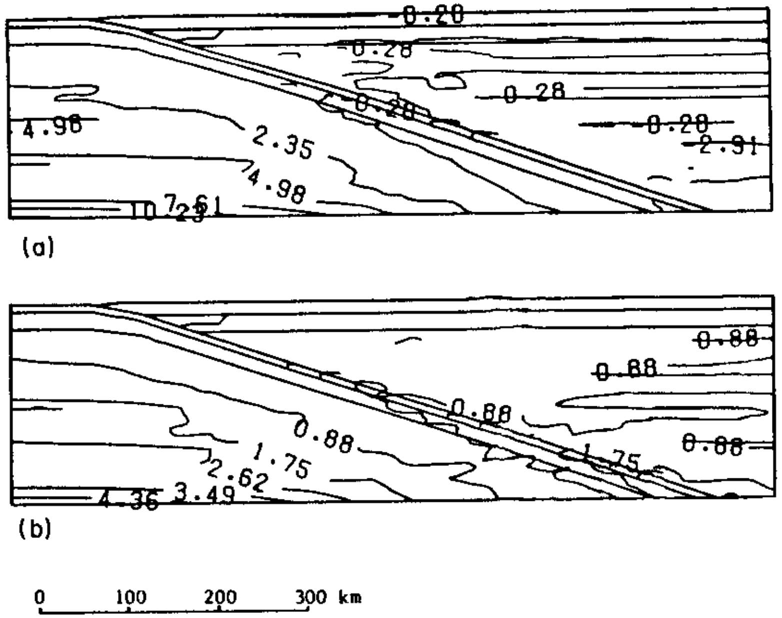

FIG. 13. (*a*) Average stress distribution of gravitational model. (*b*) Maximum shear stress distribution of gravitational model.

If the external stresses are held constant while cracks extend, the condition for unstable equilibrium of a crack of length $2c$ in a material of thickness t is (Jaeger and Cook 1979)

$$\frac{\partial}{\partial c}(W - 4\alpha ct) = 0$$

where W is the strain energy of the body; and α is the apparent surface energy density of the fracture. For a rectangular plate of length l, width b, and thickness t, containing a flat elliptical crack of length $2c$ extending along the direction of the thickness, the strain energy W in the plate for conditions of plane strain is

$$W = W_0 + \pi c^2 t(1 - \nu^2)(\sigma_n^2 + \tau^2)/E$$

where W_0 is the strain energy of the plate without the crack; E is intrinsic Young's modulus; ν is Poisson's ratio; σ_n is normal stress, which is perpendicular to the crack; and τ is the shear stress parallel to the crack. In the case of a closed crack, the effective stress ($|\tau| - \sigma_n \tan\phi$) is the only component of stress free to generate additional strain energy around the crack. Hence, the strain energy of the body can be obtained by substituting $\sigma_n^2 + \tau^2$ for the effective stress. If the cracks are randomly oriented, a spherical average may be taken over all directions, and this yields a factor of 1/3. The strain energy can then be written as

$$W = W_0 + \pi c^2 t(1 - \nu^2)(|\tau| - \sigma_n \tan\phi)^2/3E$$

The crack will be begin to grow when

$$c \geq 2\alpha E/\pi(1 - \nu^2)(|\tau| - \sigma_n \tan\phi)^2$$

Assume the cracks of various size distribute as (Fig. 11)

$$P_0(c) = 2c/\sigma^2 \cdot \exp(-c^2/\sigma^2)$$

This distribution has a similar form to a normal distribution, but $P_0(c) = 0$ when $c = 0$.

If the rock contains only one crack, and the size is controlled by P_0, the probability that the crack in the rock will begin to grow under stress $|\tau| - \sigma_n \tan\phi$ is given by the probability that the crack is longer than critical. Therefore, the probability that the crack will not break is

$$1 - \int_c^{\infty} 2c/\sigma^2 \cdot \exp(-c^2/\sigma^2)dc = 1 - \exp(-c^2/\sigma^2)$$
$$= 1 - \exp(-\lambda^2/\sigma^2 S^4)$$

where $\lambda = 2\rho\alpha E/\pi(l - \nu^2)$; and $S = |\tau| - \sigma_n \tan\phi$. However, a body usually has a lot of cracks within it. The idea that one part of the body is more stable than another suggests that the probability of failure of the cracks within a certain volume of the body is smaller than within other parts. If we assume the body contains n cracks per unit volume, we will assume part of the body fails if at least one of those cracks begins to grow. Therefore, the probability ($1 - P$) that no cracks within the unit volume will begin to grow under stress $|\tau| - \sigma_n \tan\phi$ is the product of the probability that an individual crack will not begin to grow, i.e.,

$$1 - P = (1 - P_0)^n$$
$$= [1 - \exp(-\lambda^2/\sigma^2 S^4)]^n$$

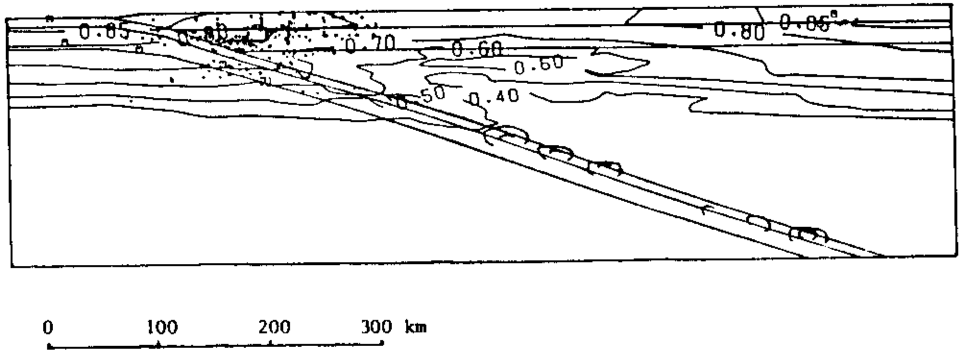

FIG. 14. Distribution of instability for model under gravitational load.

This gives (Fig. 12)

$$P = 1 - [1 - \exp(\lambda^2/\sigma^2 S^4)]^n$$

Because λ and σ are unknown, it is generally convenient to introduce a relative measurement that will indicate that one area is closer to failure than another.

Different values of λ, σ, and n do not change the basic shape of the curve of the probability function. The parameter $n = 1$ implies that for a volume V of a body that contains one crack per unit volume, the probability of any one of these cracks failing is

$$1 - 1 - \exp(-\lambda^2/\sigma^2 S^4)^V$$

From this we get the physical notion that the strength of such a cracked body decreases exponentially with volume. If $n \neq 1$, this qualitative relation is conserved. The only justification for the choice of these constants is to make the curve have a reasonable shape as normalized S changes from 0 to 1. We chose 0.116 and 1 for λ^2/σ^2 and n, respectively. The frictional angle ϕ was chosen as 30°.

Instability analysis for Vancouver Island region

Using a 1300 element model (Fig. 11), the first test was calculated assuming only gravitational load. The model is restricted to move in the vertical direction only on both left and right sides; on the bottom, no displacement can take place. Residual stress is derived by subtracting an assumed gravitational stress field due to an infinite homogeneous half-space from the stress field calculated by the model (Uribe-Carvajal 1984). Figure 13*a* shows the average stress $(\sigma_1 + \sigma_3)/2$. Figure 13*b* shows the maximum shear stress $(\sigma_1 - \sigma_3)/2$. The normal stress field due to an infinite homogeneous half-space was calculated by assuming density $\rho = 3.0$ g/cm³ and Poisson's ratio $\nu = 0.3$. In Fig. 13*b*, some contours concentrate along the lower part of the subducting plate.

The instability was calculated by means of effective stress. Figure 14 shows the distribution of the instability of the Vancouver Island region. The contours of equal instability show that the instability concentrates along the subducting slab. This implies that the sinking slab is more unstable than its surrounding regions, and earthquakes will have a greater probability of occurring within those regions. This phenomenon agrees with the concept of the Benioff zone and the general idea that earthquakes occurring along the Benioff zone are probably due to the gravitational stress. Unfortunately, the area beneath Vancouver Island, a region with anomalous structures and seismicity, lacks such instability concentration.

The stress introduced by the ridge push is about 200×10^5 Pa (200 bar), and a resistance force of the order of 20×10^5 Pa (20 bar) will be generated along the plate boundary. Generally, the materials along the plate boundary do not behave elastically; creep will occur in this region. Unfortunately, our finite-element technique cannot yet deal with such a discontinuity boundary, and the scale of our finite-element model is not big enough to introduce a transition layer with a small Young's modulus along the boundaries. We have assumed strong coupling. Kanamori (1977) suggested that shallow subduction, such as occurs along the Juan de Fuca plate, will result in a strong coupling between oceanic and continental lithosphere. The tight coupling built into our model will give an approximation for the situation of Vancouver Island. The second model was calculated for the case when there is an external force, from ridge push, exerted on the oceanic plate. In this model, we assume a 20×10^5 Pa (20 bar) viscous force acting on the oceanic plate from the upper mantle opposing the motion of the plate. At the convergent margin, an additional 20×10^5 Pa (20 bar) frictional force acts on the top of the oceanic plate.

Figure 15 shows the instability distribution of the model and the distribution of the earthquakes that have occurred in that region. By comparing Fig. 14 with Fig. 15, it can be seen that the zone located beneath Vancouver Island became more unstable. The unstable zone that is enclosed by the contours can also be recognized by the fact that the earthquake foci concentrate in that region. The observed seismicity occurring in the area is one of the constraints on the model.

The force from mantle convection can also be considered as a possible driving force for the motion of the oceanic plate. In the next model, we assumed that there is about 10^6 Pa (10 bar) viscous force on the base of the oceanic plate. This will give the effect that mantle convection is actively involved in the driving mechanism. Figure 16 shows the distribution of the instability for this model. Again in this model, the contours are

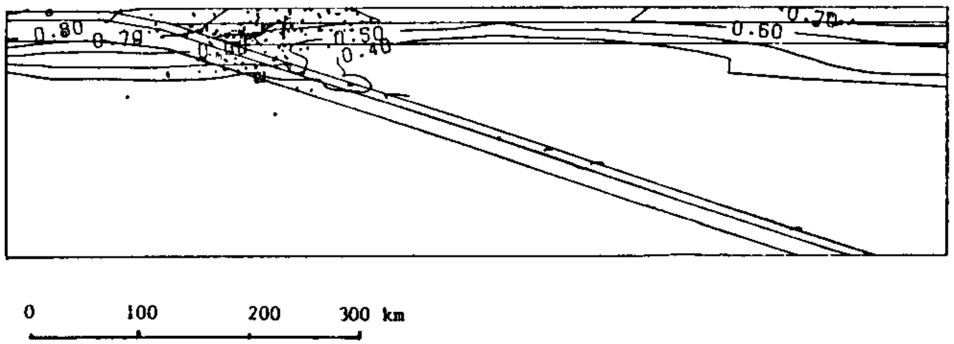

FIG. 15. Instability distribution for model with ridge-push force exerted on oceanic plate.

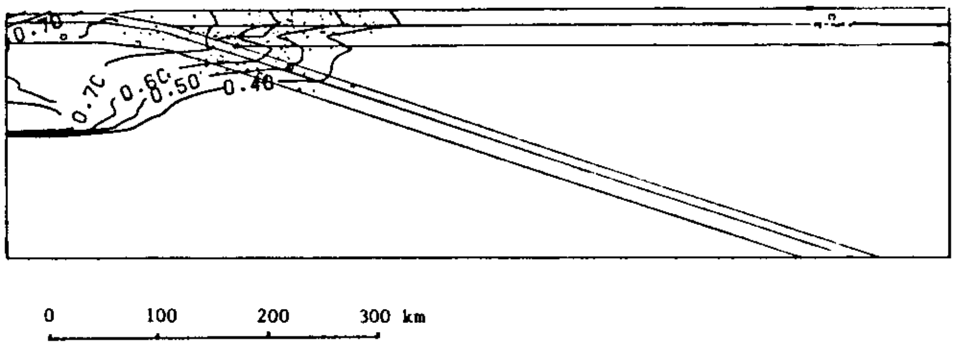

FIG. 16. Distribution of instability for model with an active viscous drag on the bottom of the oceanic plate by the asthenosphere.

concentrated on the top of the subducting plate. The contours with values of 0.4, 0.5, and 0.6 are all concentrated in the region located beneath Vancouver Island, and they do not show up at the right side of the model or at the deep part of the subducting plate. This result implies that under the applied force from gravitational ridge pushing and mantle convection, the region located beneath Vancouver Island is more unstable than the rest of the model.

Conclusions

Comparing the instability analysis in models 1, 2, and 3, one of the things we should notice is that the unstable zone at the top of the subducting plate, located beneath Vancouver Island, is probably caused by stress due to ridge push and mantle convection. The gravitational pull of the dense subducted slab does not seem to affect that region very much. If this is true, the state of the tectonic stress of that region, caused by interaction between the oceanic plate and the continental plate under the forces due to ridge push and mantle convection, should be predominantly horizontal. If this is correct, it should influence the focal mechanism of normal depth earthquakes in the Vancouver Island region.

The downward stress in the area, deduced from earthquake focal mechanisms, is north–south compressive (Rogers 1979). The plate motion is northeast, and the perpendicular to the Juan de Fuca ridge points slightly south of east. Clearly, the dyanmics of the area are complex and should be modelled in three dimensions. The ridge-push force we consider is a component of the true force in the direction perpendicular to the subduction zone. It is the component parallel to the direction of plate motion and probably contains components of mantle interaction. Until a three-dimensional model of this area is built, the interpretation of the model results should be approached with caution.

Although it is accepted by most geophysicists and geologists that the Explorer and Juan de Fuca plates subduct beneath Vancouver Island, the lack of a Benioff earthquake zone is still controversial. The lack of a Benioff zone in the Vancouver Island region would suggest that no such gravitational pull acts on the deep part of the subducting plate. Heat flow in southwest British Columbia suggests that one of the possible reasons for high heat flow farther inland could be the upwelling of magma and the convective transport of heat from a sinking slab. Melting may commence when the slab reaches a depth of about 100 km. The area below the critical temperature for earthquakes is above 70 km in the sinking slab (Keen and Hyndman 1979). Riddihough and Hyndman (1976) also suggested that the earthquakes occur in the limited depth where the core of the subducting plate remains cool and allows brittle fracture. Because the sinking slab starts to melt at such a shallow depth, it will not generate a pulling force on the top plate. Taber and Smith's (1985) study on the focal mechanism of the earthquakes in western Washington suggested that shallow events at the top of the subducting plate may be due to body forces within the plate as the plate is pulled down by gravity. Davies (1980) discussed other factors, such as resistance at the leading edge of a slab and mantle resistance, that could oppose gravitational pull. These are forces from great depths, which are not considered in our model.

Acknowledgments

This work was carried out with support from the Natural Sciences and Engineering Research Council of Canada. We are grateful for access to unpublished information on the thermal and gravity models of T. Lewis and J. F. Sweeney.

DAVIES, G. F. 1980. Mechanics of subducted lithosphere. Journal of Geophysical Research, 10, pp. 6304–6318.

ELLIS, R. M., SPENCE, G. D., CLOWES, R. M., WALDRON, D. A., JONES, I. F., GREEN, A. G., FORSYTH, D. A., MAIR, J. A., BERRY, M. J., MEREU, R. F., KANASEWICH, E. R., CUMMING, G. L., HAJNAL, Z., HYNDMAN, R. D., MCMECHAN, G. A., and LONCAREVIC, B. D. 1983. The Vancouver Island Seismic Project: a CO-CRUST onshore–offshore study of a convergent margin. Canadian Journal of Earth Sciences, 20, pp. 719–741.

GREEN, A. G., CLOWES, R. M., YORATH, C. J., SPENCER, C., KANASEWICH, E. R., BRANDON, M. T., and BROWN, A. S. 1986a. Reflection mapping underplated oceanic lithosphere and the subducting Juan de Fuca plate. Nature (London), 319, pp. 210–213.

GREEN, A. G., BERRY, M. J., SPENCER, C. P., KANASEWICH, E. R., CHIU, S., CLOWES, R. M., YORATH, C. J., STEWART, D. B., UNGER, J. D., and POOLE, W. H. 1986b. Recent seismic reflection studies in Canada. American Geophysical Union, Geodynamics Series, Vol. 13, pp. 85–97.

JAEGER, J. C., and COOK, N. G. W. 1979. Fundamentals of rock mechanics. Fletcher & Sons Ltd., Norwich, England.

KANAMORI, H. 1977. Seismic and aseismic slip along subduction zones and their tectonic implications. *In* Island arcs, deep-sea trenches and back-arc basins. *Edited by* M. Talwani and W. C. Pitmann, III. American Geophysical Union, Maurice Ewing Series 1, pp. 163–174.

——— 1980. The state of stress in the Earth's lithosphere. *In* Physics of the Earth's interior. *Edited by* A. M. Dziewonski and E. Boschi. North-Holland Co., Amsterdam, The Netherlands, pp. 531–552.

KEEN, C. E., and HYNDMAN, R. D. 1979. Geophysical review of the continental margins of eastern and western Canada. Canadian Journal of Earth Sciences, 16, pp. 712–747.

KIRBY, S. H. 1977. State of stress in the lithosphere: inference from flow laws of olivine. Pure and Applied Geophysics, 115, pp. 245–258.

LEEDS, D. K., KAUSEL, E. G., and KNOPOFF, L. 1974. Variations of upper mantle structure under the Pacific Ocean. Science, 186, pp. 141–143.

LI, Q. 1986. Analysis of instability of the Vancouver Island lithoprobe transect. M.Sc. thesis, University of Alberta, Edmonton, Alta.

MCKENZIE, D. P. 1969. Plate tectonics. *In* The nature of the solid Earth. *Edited by* E. C. Robertson. McGraw-Hill, New York, NY, pp. 742–752.

MCMECHAN, G. A., and SPENCE, G. D. 1983. *P*-wave velocity structure of the Earth's crust beneath Vancouver Island. Canadian Journal of Earth Sciences, 20, pp. 742–752.

MILNE, W. G., ROGERS, G. C., RIDDIHOUGH, R. P., MCMECHAN, G. A., and HYNDMAN, R. D. 1978. Seismicity of western Canada. Canadian Journal of Earth Sciences, 15, pp. 1170–1193.

MOLNAR, P., FREEDMAN, D., and SHIH, J. 1979. Lengths of intermediate and deep seismic zones and temperatures in downgoing slabs of lithosphere. Geophysical Journal of the Royal Astronomical Society, 56, pp. 41–54.

RIDDIHOUGH, R. P. 1977. A model for recent plate interactions off Canada's west coast. Canadian Journal of Earth Sciences, 14, pp. 384–396.

——— 1979. Gravity and structure of an active margin—British Columbia and Washington. Canadian Journal of Earth Sciences, 16, pp. 359–363.

——— 1984. Recent movements of the Juan de Fuca plate system. Journal of Geophysical Research, 89, pp. 6980–6994.

RIDDIHOUGH, R. P., and HYNDMAN, R. D. 1976. Canada's active western margin: the case for subduction. Geoscience Canada, 3, pp. 384–396.

ROGERS, C. C. 1979. Earthquake fault plane solutions near Vancouver Island. Canadian Journal of Earth Sciences, 16, pp. 523–531.

STACEY, R. A. 1973. Gravity anomalies, crustal structure, and plate tectonics in the Canadian Cordillera. Canadian Journal of Earth Sciences, 10, pp. 615–628.

STACEY, F. D. 1977. Physics of the Earth. 2nd ed. John Wiley & Sons, New York, NY.

TABER, J. J., and SMITH, S. W. 1985. Seismicity and focal mechanisms associated with the subduction of the Juan de Fuca plate beneath the Olympic Peninsula, Washington. Bulletin of the Seismological Society of America, 75, pp. 237–249.

TURCOTTE, D. L. 1974. Are transform faults thermal contraction cracks? Journal of Geophysical Research, 79, pp. 2573–2677.

URIBE-CARVAJAL, A. 1984. Seismic stability studies near the Middle America Trench. Ph.D. thesis, University of Alberta, Edmonton, Alta.

WATTS, A. B., BODINE, J. H., and STECKLER, M. S. 1980. Observations of flexure and the state of stress in the oceanic lithosphere. Journal of Geophysical Research, 85, pp. 6369–6376.

WIENS, D. A., and STEIN, S. 1983. Age dependence of oceanic intraplate seismicity and implications for lithospheric evolution. Journal of Geophysical Research, 88, pp. 6456–6468.

YORATH, R. M., CLOWES, R. M., BROWN, A. S., BRANDON, M. T., MASSEY, N. W. D., GREEN, A. G., SPENCER, C., KANASEWICH, E. R., and HYNDMAN, R. D. 1985. Lithoprobe phase 1: southern Vancouver Island: preliminary analyses of reflection seismic profiles and surface geological studies. *In* Current research, part A. Geological Survey of Canada, Paper 85-1A, pp. 543–554.